POLYMERIC COMPOSITES FILLED WITH CELLULOSE MICRO- AND NANOCRYSTALS FOR THE RESTORATION OF CELLULOSE-BASED ARTWORKS: CHARACTERIZATION AND APPLICATION

A.Cataldi[1], F.Deflorian[1], A.Pegoretti[1]

[1]University of Trento, Department of Industrial Engineering
Via Sommarive 9, Povo - 38123 Trento (Italy)
annalisa.cataldi@unitn.it
flavio.deflorian@unitn.it
alessandro.pegoretti@unitn.it

Keywords: Cellulose, composites, mechanical properties, wood, adhesion

Abstract
Micro- and nanocomposites based on thermoplastic resins, widely used in the restoration (Paraloid® B72 a consolidant of damaged wood, and Aquazol® 500 an adhesive for the oil paintings lining) were filled with microcrystalline cellulose (MCC) and aqueous suspension of cellulose nanocrystals (CNC) in order to improve their thermo-mechanical properties. The extended characterizion on these materials showed how both MCC and CNC promoted a stabilizing effect on the neat matrices with an increment of the elastic modulus and a reduction of the thermal expansion coefficient and the creep compliance. Micro- and nanocomposites adhesive films of Aquazol 500 were applied between to canvases in order to simulate the lining restoration of oil paintings. Single-lap shear tests confirmed the increase of the dimensional stability of the polymer after the MCC and CNC addition upon to long lasting creep stresses. In particular, the introduction of CNC led to a better thermo-mechanical response of nanocomposites with respect to microcomposites. Paraloid microcomposites were applied as consolidants of historical worm-eaten walnut wood samples, reporting an effective recovering of the elastic modulus, mechanical strength and surface hardness in comparison to damaged untreated samples.

1. Introduction

Thermoplastic polymers are commonly utilized for the conservation of cultural heritage. Among these resins, Paraloid B72 is certainly one of the most famous and selected products by conservators. This MA/EMA copolymer, thanks to its good optical features, high chemical stability and yellowing and photo-oxidation resistance is applied as protective material for metals and stones, consolidant for wood and also as adhesive or varnish in the restoration of paintings [1, 2]. Another versatile polymer quite utilized by conservators is Aquazol 500, a poly (2-ethyl-2-oxazoline), generally called PEOX, soluble in water and in a wide range of other organic solvents. Aquazol is mainly used as adhesives for several classes of artworks [3, 4]. Natural fillers present several advantages in comparison to their corresponding synthetic reinforcing agents. They are non-toxic, biodegradable and recyclable. Natural plant derived particles have generally lower density and high specific strength and elevated stiffness. Microcrystalline cellulose MCC, is one of the most used reinforcing fillers, it can be easily prepared through the reaction of cellulose with water solution of strong mineral acid at boiling temperature. The hydrolysis reaction removes the amorphous fraction and reduces the degree of polymerization of the cellulose chains [5]. Cellulose nanocrystals, CNC, are produced by the acid hydrolysis of natural cellulose sources [6]. Still and rod-like CNC particles have interesting properties, in terms of biocompatibility, anisotropy, good optical transparency, low thermal expansion coefficient and, especially, high elastic modulus, similar to steel [7]. These

Excerpt from ISBN 978-3-00-053387-7

features guarantee to cellulose based fillers a wild range of applications and promising results in the composite technology. The final aim of this research is the improvement of the mechanical performance of commercial resins (i.e. Paraloid B72 and Aquazol 500), especially in terms of dimensional stability, strength and elastic modulus, developing micro- and nanocomposites with a lower environmental impact and interesting functional properties more suitable for restoration works.

2. Experimental

2.1. Materials

Paraloid B72 (PB72) produced by Rohm and Hass (Germany), with a specific gravity of 1.15 $g \cdot cm^{-3}$, and a poly (2-ethyl-2-oxazoline), Aquazol 500 (AQ500), with a specific density of 1.07 $g \cdot cm^{-3}$ supplied by Polymer Chemistry Innovation (USA) were selected as polymeric matrices. A microcrystalline cellulose (MCC), in form of fine powder, supplied by Sigma Aldrich (USA), with a specific gravity of 1.56 $g \cdot cm^{-3}$ and average aspect ratio of 2.4 was selected as reinforcing agent. Aqueous suspensions of cellulose nanocrystals (CNC), kindly supplied by the Wallenberg Wood Science Center (Stockholm, Sweden), with an average aspect ratio of 50 were used as nanofiller.

2.2. Preparation of micro- and nanocomposites

Microomposites based on PB72 and AQ500 were melt-compounded in a Haake Rheomix® internal mixer (t= 160 °C, rotor speed=60 rpm, t= 5 min) and compression molded in a Carver hydraulic press (T= 160°C, p= 4 MPa, t= 5 min), with different MCC amounts from 5 wt% to 30 wt%. Using an aqueous solution at 5 wt% of AQ500 and aqueous suspensions at 5.5 wt% and 8.7 wt% of cellulose nanocrystals as filler, nanocomposites with a CNC content of 5 wt% and 30 wt% were produced by solution mixing and film casting. Microcomposites made of AQ500 and MCC were produced through the same method. All MCC and CNC formulations were dried at 40 °C in a vacuum oven until the complete cleaning of the solvent. In this way films with an average thickness of 250 μm were obtained. Before testing, samples were dried at 50 °C for 24 h in a vacuum oven.
All micro- and nanocomposite samples were denoted indicating the matrix (AQ500), the type of filler (MCC or CNC) and its weight amount. For instance, AQ500-MCC-5 represents a sample with a mcc content of 5 wt%. While, AQ500-CNC-5 identifies a composite with a CNC amount of 5 wt%.

2.3. Production of adhesive joints

Adhesive joints (12.7 mm long and 25 mm wide) connecting two kinds of canvas, an English linen (170 g/m^2), representing the original oil painting substrate, and a woven polyester (260 g/ m^2) utilized as lining textile, were obtained by using a temperature of 65°C and a pressure of 1MPa for 5 min. In this way rectangular samples 200 mm long and 25 mm wide were produced to be tested by single-lap shear test. Before testing, samples were conditioned at 23°C and 55% of relative humidity in a chamber with a super-saturated solution of $Mg(NO_3)_2 \cdot 6H_2O$ for 48 hours.

2.4. Application of PB72 microcomposites as consolidants for worm-eaten wood

Acetone solutions at 10 wt% of neat PB72 and corresponding PB72/MCC composites with a filler content of 5 wt% and 30 wt% were applied by brush on degraded walnut wood samples (5X5X80 mm^3). An amount of around 130 mg of consolidating solutions was utilized on each face of rectangular samples. All samples were air-dried to allow the solvent removal and before testing they were conditioned at 23°C and 55% of relative humidity in a chamber with a super-saturated solution of $Mg(NO_3)_2 \cdot 6H_2O$ until the equilibrium point was reached.

Excerpt from ISBN 978-3-00-053387-7

2.5. Experimental techniques

Dynamic mechanical thermal analysis (DMTA) and Creep tests were performed by using DMA Q800 device by TA Instruments under tensile configuration. Rectangular specimens 15 mm long, 5 mm wide and 1.3 mm thick were tested in a temperature range between -10 °C and 150 °C at a heating rate of 3 °C·min^{-1} and a frequency of 1 Hz to determine the trends of the storage modulus (E'), loss modulus (E") and loss tangent (tanδ) as a function of the temperature. Moreover, through the evaluation of the thermal strain it was possible to determine the coefficients of linear thermal expansion (CLTE) below Tg (i.e. in a temperature interval between 0 °C and 55 °C for MCC filled composites and between 0 °C and 40 °C for CNC filled samples) and above Tg (between 60 °C and 70 °C for MCC based composites and between 70 °C and 80 °C for CNC filled samples). While, applying a constant stress (σ_0= 10% of the stress at break, σ_B of the neat matrices) at 30 °C for a total time of 3600 s the creep compliance D(t), calculated as the ratio between the time dependent deformation ε(t) and the applied stress, was evaluated. Quasi-static tensile tests were carried out on melt-compounded microcomposites (gage length= 25 mm) by means of a universal tensile testing machine Instron® 4502, with a load cell of 1kN and a crosshead speed of 10 mm/min. At least five specimens for each formulation were tested in order to determine the tensile strength σ_B, the maximum strain at break ε_B, and the elastic modulus E. Single-lap shear tests in quasi-static and creep conditions were performed on rectangular canvas samples (gage length= 130 mm, width= 25 mm) by using an Instron® 4502 universal testing machine, equipped with a 10kN load cell, at crosshead speed of 10 mm/min to determine the adhesive shear strength (τ_B), by dividing the maximum force for the overlapping area. While the time depending joint displacement (u), was obtained applied a constant stress (τ_0), corresponding to about 50% of the shear stress at break (τ_B) of the neat matrix for 3600 s. At least five specimens of each formulation were tested for each test. Three points bending tests were performed on intact and damage walnut wood samples untreated and treated with PB72/MCC microcomposites solutions (gage length= 140 mm) by using an Instron® 4502 equipped with a load cell of 5 kN and a crosshead speed of 1.3 mm/min. Shore D hardness tests were conducted on the same samples mechanically tested. Thanks to the optical microscope observations of the surfaces and the longitudinal sections of all samples it was possible to estimate the penetration level of consolidant solutions and microcellulose.

3. Results and Discussions

3.1. DMTA

In Table 1-2 the storage (E') and loss (E") moduli, loss factor (tanδ) and glass transition temperature (Tg) values of micro- and nanocomposites based on PB72 and AQ500 are reported. Micro- and nanocellulose play a similar and interesting effect on both matrices with a progressive increase of the dynamic moduli that corresponds to an increment of the stiffness as the micro- and nanofiller content increases. Additionally, only for nanocomposites one can notice an increment of the Tg up to 10 degrees for AQ500 after the introduction of the highest amount of CNC (Table 2).

Table 1. Results of DMTA tests on neat Paraloid and resulting microcomposites.

Samples	**E' at 25°C (GPa)**	**E" peak value (GPa)**	**tanδ peak value**	**Tg from E" (°C)**
PB72	**2.04**	**0.29**	**2.01**	**50.5**
PB72-MCC-5	**2.32**	**0.34**	**1.95**	**50.1**
PB72-MCC-30	**2.85**	**0.46**	**1.70**	**49.3**

Excerpt from ISBN 978-3-00-053387-7

Table 2. Results of DMTA tests on neat Aquazol 500 and resulting micro- and nanocomposites

Samples	**E' at 25°C (GPa)**	**E" peak value (GPa)**	**tanδ peak value**	**Tg from E" (°C)**
AQ500	**1.86**	**0.41**	**3.21**	**72.0**
AQ500-MCC-5	**2.53**	**0.53**	**2.16**	**69.1**
AQ500-MCC-30	**4.60**	**0.96**	**0.84**	**68.9**
AQ500-CNC-5	**3.06**	**0.70**	**2.23**	**74.7**
AQ500-CNC-30	**6.86**	**1.33**	**0.78**	**82.6**

While, the determination of the coefficient of linear thermal expansion (CLTE), calculated, as the slope of the secant line of thermal strain curves in the glassy ($CLTE_g$) and rubbery ($CLTE_r$) states (Figure 1(a-b)), underlines how the introduction of MCC and CNC leads to the improvement of the dimensional stability of the neat matrices with a decrease of CLTE proportional to the filler amount under and above the glass transition temperature. As one can see, the effect played by CNC nanoparticles on the viscoelastic behavior of the resulting materials is much more pronounced than that obtained for MCC filled composites.

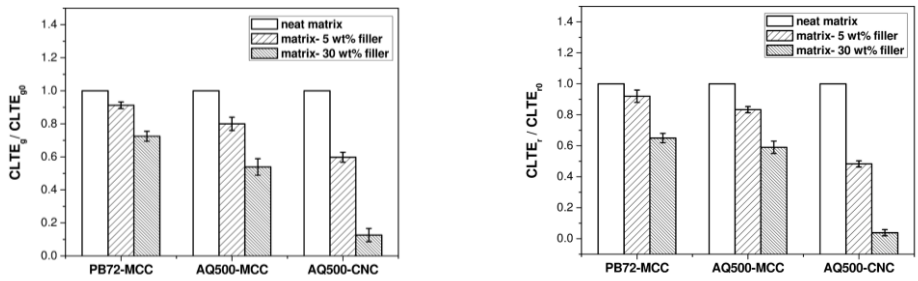

(a) (b)

Figure 1. Relative trends of linear thermal expansion coefficients of MCC and CNC polymer composites. (a) Coefficient of linear thermal expansion below T_g, $CLTE_g$, (b) coefficient of linear thermal expansion above T_g, $CLTE_r$.

3.2. Creep tests

The stabilizing effect provided by MCC and CNC particles is confirmed by creep test. In fact, as reported in Figure 2(a-c), the creep compliance of the neat matrices is significantly reduced at elevated filler contents, especially for long creep times.

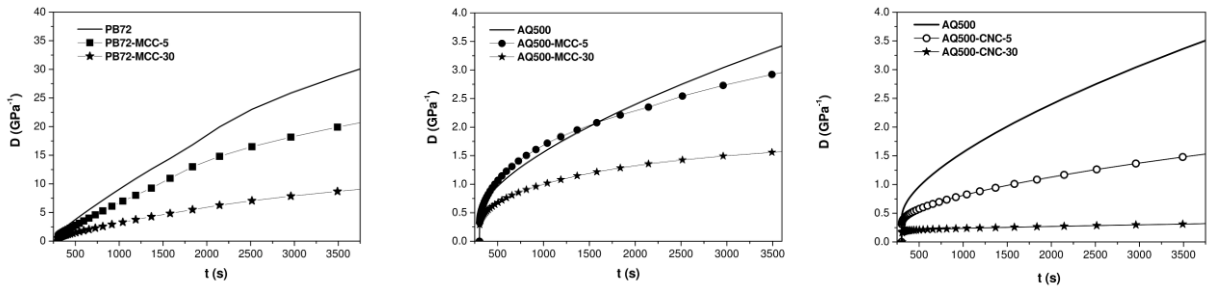

(a) (b) (c)

Figure 2. Representative creep compliance D, curves of (a) Paraloid and corresponding microcomposites, (b) Aquazol and corresponding microcomposites, (c) Aquazol and corresponding nanocomposites.

Excerpt from ISBN 978-3-00-053387-7

In Figure 3 the relative trend of creep compliance D, is showed. It is interesting to note how, also in these tests, CNC nanocomposites registered the highest enhancement of the dimensional stability with respect to MCC filled formulations.

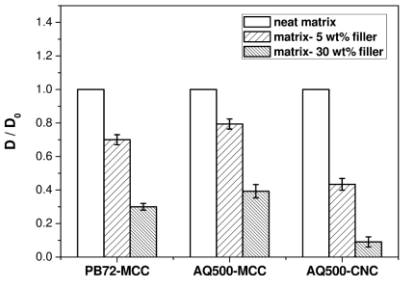

Figure 3. Relative creep compliance trends of Paraloid and Aquazol composites.

3.3. Quasi-static tensile tests

Tensile tests were performed on Paraloid and Aquazol based composites filled with MCC. In this way the elastic modulus E, and the ultimate tensile properties, maximum stress at break σ_B, and the maximum strain at break ε_B were estimated (Table 3).

Table 3. Main results from tensile tests of Paraloid and Aquazol microcomposites.

Samples	**E (GPa)**	**σ_B (MPa)**	**ε_B (%)**
PB72	**1.65 ± 0.06**	**23.53 ± 0.39**	**2.49 ± 0.11**
PB72-MCC-5	**1.71 ± 0.06**	**24.60 ± 0.38**	**2.78 ± 0.01**
PB72-MCC-30	**3.13 ± 0.09**	**35.82 ± 1.88**	**2.50 ± 0.13**

Samples	**E (MPa)**	**σ_B (MPa)**	**ε_B (%)**
AQ500	**11.56 ± 0.20**	**3.90 ± 0.21**	**724 ± 29**
AQ500-MCC-5	**14.31 ± 0.70**	**4.13 ± 0.09**	**646 ± 14**
AQ500-MCC-30	**38.68 ± 1.44**	**5.90 ± 0.10**	**276 ± 8**

The results reported in Table 3 show that MCC is able to considerably rise the elastic modulus and therefore the stiffness of both matrices with the increasing of the filler content. Interestingly, also the tensile strength of PB72 and AQ500 increases proportional to the MCC loading. While, if the strain at break of PB72 is not affected by the presence of MCC, AQ500 exhibits the stabilizing effect due to MCC through a progressive decrease of the deformation.

3.4. Single-lap shear test

Single-lap shear tests in quasi-static and creep configuration were performed on canvas samples lined by thin MCC and CNC filled films in order to verify if the positive action played by both fillers on the dimensional stability and the creep resistance of PB72 and AQ500 is visible even under end use simulated conditions. In Figure 4 (a-b) relative trends of adhesive strength τ_B, and joint displacement u, as a function of the filler content, registered by micro- and nanocomposites are depicted.

Excerpt from ISBN 978-3-00-053387-7

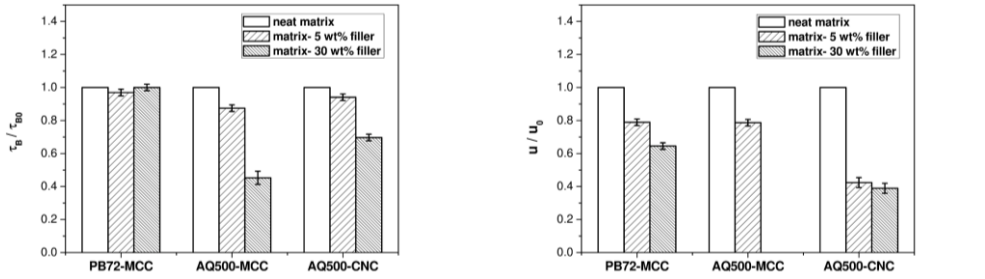

(a) (b)

Figure 4. Main single-lap shear tests results for micro- and nanocomposites (a) Relative adhesive strength trend (τ_B) (b) Relative joint displacement trend (u)

As one can see, MCC does not impair the adhesive strength of Paraloid, while for AQ500-MCC and AQ500-CNC composites a systematic decrease of this property is observed. In particular, MCC leads to the most relevant drop of τ_B upon to a reduction of about 60% at the highest filler amount in comparison to the neat matrix and against the 30% less reported by nanocomposites with 30 wt% of CNC. On the other hand, all formulations exhibit an improvement of the dimensional stability after the introduction of both MCC and CNC even during applications as lining adhesives through the reduction of the joint displacement proportionally to the filler loading. The best response is registered by nanocomposites with a decrease of u up to 60% for formulation with 30 wt% of CNC, while, microcomposites with the highest amount of MCC failed during tests because of the significant strength loss.

3.5. Three-points bending tests

Samples of untreated damaged wood (DW) and intact walnut wood (UW) and samples of worm-eaten walnut wood consolidated with pure PB72 (DW-T0), PB72 filled with 5 wt% of MCC (DW-T5) and with 30 wt% of MCC (DW-T30) were examined. The bending tests were conducted on at least 15 specimens of each group of samples. In fig. 5(a-b) the values of maximum flexural strength $\sigma_{MAX,f}$ and flexural elastic modulus E_f of all samples are represented.

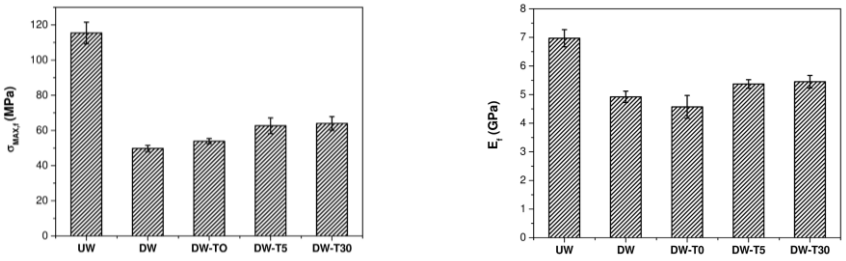

(a) (b)

Figure 5. Main results from three-points bending tests on undamaged wood (UW), dameged untreated wood (DW), dameged wood treated with PB72 (DW-T0), with PB72 e 5 wt% of MCC (DW-T5) e with composite at 30 wt% of MCC (DW-T30). (a) Maximum flexural strength $\sigma_{MAX,f}$ (b) flexural elastic modulus E_f.

It is interesting to see the dramatic drop in the mechanical properties showed by worm-eaten wood samples in comparison to the intact wood and how the treatment with Paraloid is able to partially recover this gap. Moreover, the presence of MCC makes more effective the consolidating properties of Paraloid. Wood samples treated by microcomposites exhibit the highest values of $\sigma_{MAX,f}$ and they are the only samples reporting the increase of E_f. Additionally, there are no significant differences between the mechanical responses of samples consolidate with PB72-MCC-5 and PB72-MCC-30,

Excerpt from ISBN 978-3-00-053387-7

therefore the positive effect of MCC on the mechanical behavior of this historical wood is evident since the lowest filler loading.

3.6. Surface hardness tests

The surface hardness measurements were carried out on the samples previously tested by bending tests. The Table 4 shows the values of surface hardness, H, determined in the radial H_R, and tangential H_{Tg}.

Table 4. Surface hardness values measured in the radial H_R, and tangential H_{Tg} direction of samples of intact wood (UW), untreated worm-eaten wood (DW) and treated with neat Paraloid (DW-T0), with Paraloid and 5 wt% of MCC (DW-T5)and with 30 wt% of MCC (DW-T30)

Samples	H_R	H_{Tg}
UW	**69.25 ± 0.63**	**63.51 ± 0.17**
DW	**65.56 ± 0.81**	**62.78 ± 0.64**
DW-T0	**65.70 ± 0.70**	**62.88 ± 0.80**
DW-T5	**67.44 ± 0.59**	**64.33 ± 0.79**
DW-T30	**69.03 ± 0.46**	**67.70 ± 0.42**

Also these measurements evidence an action played by MCC on the matrix. The microcellulose creates a deposit on the surface of treated samples, mainly effective at higher contents of MCC that promotes an increment of the surface hardness in both examined directions. The increase of H is proportional to the MCC loading and for samples consolidated with PB72 filled with 30 wt% of MCC the H_r and H_{tg} values are almost up to the intact wood values.

3.7. Assessment of the penetration level of consolidating composites

Thanks to optical microscope observations of the longitudinal sections of degraded walnut wood before and after treatments with PB72/MCC composites solutions (Fig. 6), it is possible to notice that the presence of microcellulose does not affect the penetration capability of the neat product.

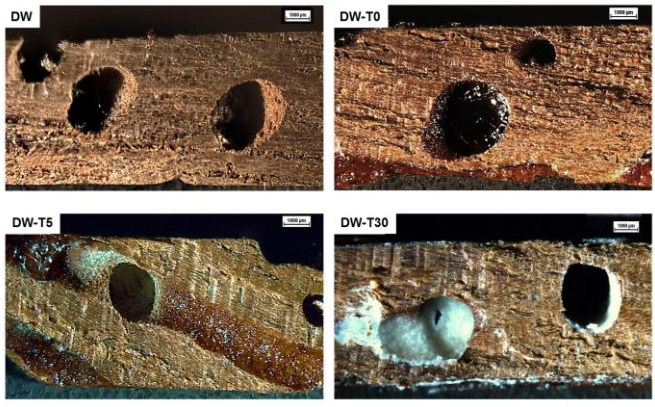

Figure 6. Optical microscope images of longitudinal sections of damaged wood untreated (DW) and treated with neat Paraloid (DW-T0), with Paraloid and 5 wt% of MCC (DW-T5) and with 30 wt% of MCC (DW-T30)

Actually, white deposits of microcellulose, more abundant at higher filler amount, are visible together with the polymer into the holes and galleries made by worm larvae. This evidence explains the good mechanical results reported by filled PB72 based consolidations.

Excerpt from ISBN 978-3-00-053387-7

4. Conclusions

Innovative micro- and nanocomposites were produced starting from thermoplastic resins, widely used in the restoration works, and adding a microcrystalline cellulose (MCC) and aqueous suspensions of cellulose nanocrystals (CNC), as reinforcing agents. Thermal analysis highlighted how the introduction of both MCC and CNC led to a stabilizing effect on the neat matrices, promoting the increment of the elastic modulus and the reduction of the linear thermal expiation coefficient and the creep compliance. Only for microcomposites it was possible to evaluate the increase of the tensile strength due to the MCC presence and proportional to its filler content. These positive results oriented the application of Aquazol based micro- and nanocomposites as adhesives for the oil paintings lining. Single-lap shear tests under quasi-static and creep conditions underlined the improvement of the dimensional stability of the neat adhesive after the MCC and CNC introduction with a significant reduction of the joint displacement as the filler loading increased. Interestingly, the stabilizing effect of CNC on Aquazol 500 was more pronounced than that one produced by MCC. Moreover, acetone solutions at 10 wt% of PB72/MCC composites were applied as consolidants of worm-eaten walnut wood samples. The filled PB72 composites produced an increase of the flexural strength, the flexural elastic modulus and the surface hardness of damaged wood proportionally to the filler content.

Acknowledgments

Prof. Lars Berglund and the Wallenberg wood science center in Stockholm (Sweden) are kindly acknowledged for supplying the cellulose nanocrystals suspensions utilized in this work.

References

[1] D. Sale, Yellowing and Appearance of Conservation Adhesives for Poly(methyl methacrylate): A Reappraisal of 20-Year-Old Samples and Test Methods, *Adhesives and Consolidants for Conservation Ottawa, Canada*, 2011.

[2] S. Chapman and D. Mason, Literature Review: The Use of Paraloid B-72 as a Surface Consolidant for Stained Glass, *Journal of the American Institute for Conservation*, vol. 42, pp. 381-392, 2003.

[3] R. C. Wolbers, Short Term Mechanical Properties of Adhesives: Solvent and Plasticizer Effects, *Third Congress on Color and Conservation, Materials and Methods of Restoration of Movable Polychrome Works*, *Milan*, 2006, pp. 111-118.

[4] R. C. Wolbers, M. McGinn, and D. Duerbeck, Poly(2-Ethyl-2-Oxazoline): a new conservation consolidant, *AIC-WAG proceedings: Painted Wood: history and conservation*, 1994, pp. 514-527.

[5] P. Thummanukitcharoen, S. Limpanart, and K. Srikulkit, Preparation Of Organosilane Treated Microcrystalline Cellulose (Simcc) And The Polypropylene/ Simcc Composite, *18th International Conference On Composite Materials*, *Jeju Island, Korea*, 2011.

[6] J. F. Revol, H. Bradford, J. Giasson, R. H. Marchessault, and D. G. Gray, Helicoidal self-ordering of cellulose microfibrils in aqueous suspension, *International Journal of Biological Macromolecules*, vol. 14, pp. 170–172, 1992.

[7] J. P. F. Lagerwall, C. Schütz, M. Salajkova, J. Noh, J. H. Park, G. Scalia, *et al.*, Cellulose nanocrystal-based materials: From liquid crystal self-assembly and glass formation to multifunctional thin films, *NPG Asia Materials*, vol. 6, 2014.

Excerpt from ISBN 978-3-00-053387-7